Environmental Science and Pollution Research (2023) 30:40174–40188
https://doi.org/10.1007/s11356-022-25097-9

RESEARCH ARTICLE

Microwave-assisted synthesis of ZnO nanoparticles using different capping agents and their photocatalytic application

Kumar Mageswari[1] · Peethambaram Prabukanthan[1] · Jagannathan Madhavan[2]

Received: 11 July 2022 / Accepted: 28 December 2022 / Published online: 6 January 2023

Abstract

This investigation reports the synthesis of ZnO nanoparticles from various sources of zinc salts via a microwave-assisted method. Furthermore, the synthesized ZnO nanoparticles were capped with different capping agents such as sodium hexametaphosphate (SHMP), polyvinylpyrrolidone (PVP), and cetylpyridinium chloride (CPC) to examine the stability and characteristics of ZnO nanoparticles. The synthesized ZnO nanoparticles were characterized with sophisticated analytical techniques such as XRD, FTIR, SEM, UV–vis DRS, Raman, and PL to understand their properties. From these studies, the XRD depicts the decrease in crystallinity of ZnO nanoparticles with the addition of different capping agents, and the morphology of the ZnO nanoparticles was influenced by capping agents as evidenced by SEM. The band gap of the synthesized ZnO nanoparticles is found to decrease with different capping agents confirmed by UV–Vis DRS studies. Furthermore, the photocatalytic degradation performance of the prepared samples is assessed by the degradation of methylene blue under visible light irradiation. The ZnO nanoparticles synthesized from the Zinc nitrate source with SHMP capping agent show a greater extent of photocatalytic degradation efficiency than other Zinc sources. After 60 min of light, MB was observed to have degraded by about 80%, and hence, zinc nitrate is a suitable source to synthesize ZnO.

Keywords Zinc oxide · Capping agent · Microwave · Methylene blue · Photocatalytic degradation

Introduction

Metal oxide nanomaterials have interesting properties and potentially powerful applications in many fields, such as environmental remediation, sensing, microelectronics, and biomedicine. In general, the synthesis of metal oxide properties is significantly influenced by their size and shape, such as nanorods, nanospheres, nanoplates and nanobelts, nanowires, and nanoflowers (Pascariu et al. 2018; Flores et al. 2014; Zamirin et al. 2014). Recent research focuses on nanoparticles is particularly captivating their synthesis as well as applications in photocatalysis, semiconductors, photoluminescence, gas sensors, UV photodetectors, light-emitting diodes (LEDs), and solar cells (Chandrappa and Venkatesha 2012; Hsu et al 2013.). The properties of nanoparticles are tuned based on their size and shape that can be used in specific applications (Tiwari et al. 2012.). Recently, semiconductor oxides are widely used in the field of photocatalysis, one of the cost-effective and environmentally friendly methods to degrade organic pollutants from wastewater without producing any other secondary pollutants and it gains great attention due to its potential solar energy utilization. This is a process that usually proceeds with oxidation and reduction of contaminants at the interface of metal oxides (Zhu and Zhou 2019). Moreover, various metal oxides such as ZnO, TiO_2, Fe_2O_3, WO_3, and V_2O_5 with appropriate band gap energy are successfully reported as photocatalysts for the removal of organic pollutants (Chauhan et al. 2019).

Among several metal oxides, ZnO gained immense attraction due to its low cost, chemical stability, and eco-friendliness (Ameen et al. 2021). Various methods adopted to synthesise the ZnO nanoparticles such as hydrothermal, sol–gel, solvothermal, and mechano synthesis, but currently,

Responsible Editor: Sami Rtimi

✉ Peethambaram Prabukanthan
pprabukanthan76@hotmail.com

[1] Materials Chemistry Lab, Department of Chemistry, Muthurangam Government Arts College, Vellore 632002, India

[2] Solar Energy Lab, Department of Chemistry, Thiruvalluvar University, Vellore 632115, India

microwave irradiation is widely used for the synthesis of ZnO nanostructures. This method provides strong friction and collision of molecules leading to heating and greater acceleration nucleation of atoms. Temperature and concentration gradients of the reaction mixture are excluded in the irradiation process. This method is considered to be rapid, environmentally benign and energy-saving for the bulk production of nanomaterials (Lv et al. 2007.).

However, ZnO is found to be an n-type semiconductor photocatalyst with band gap energy value $E_g = \sim 2.9–3.3$ eV (Murali et al. 2019). Due to its wide band gap energy, it shows smaller absorption in visible region, covering a minimal part of the solar spectrum, yet the photocatalytic degradation efficiency of the ZnO is poor in the visible region because of its rapid recombination of photo-excited e^-/h^+ pairs (Samadi et al. 2016). Hence, several strategies like the formation of heterojunction, doping with metal and non-metals, and the formation of composite with narrow band gap semiconductors are implemented to enhance the photocatalytic activity of ZnO (Huang et al 2021). Among the various methods, doping with various capping agents can tune the photocatalytic degradation efficiency, due to the inter-particle charge transfer. In parallel with the development of capping with ZnO throughout the years, a variety of different approaches for capping have arisen.

The different capping agents were used in the synthesis of ZnO, and their effect on its performance has been studied in various research papers. There are several publications in which organic compounds have been used as the catalyst for photodegradation. For instance, Vignesh and co-workers (Vignesh et al. 2019) used the degradation rate of Cd:Ag:ZnO: PVP nanocomposite was 4.7 times higher than that of undoped ZnO by degrading MB dye within 120 min under visible-light exposures. Besides, the Cd:Ag:ZnO: PVP nanocomposites have good cycling stability for up to five successive cycles of photocatalytic degradation. Likewise, Senasu et al. 2021. Studied the ZnO/CdS nanocomposite showed an efficiency of 80% and 73% toward photodegradation of reactive red 141 (RR141) azo dye and ofloxacin (OFL) antibiotic, respectively. Also, Chankhanittha et al. 2021 worked on the synthesized 0.05ZnO/BWO heterojunction photocatalyst with the smallest size and lowest PL intensity, implying the highest electron–hole separation efficiency, exhibited the highest photoactivity of 87%, 85%, and 84%.

Recently, many attempts have been made using ZnO photocatalyst for the photodegradation of organic pollutants (Bhuvaneswari et al. 2021). But no reports on using different capping agents with various zinc sources towards the degradation of organic dyes have been reported so far. The organic capping agents in the ZnO molecular structure could be the reason for these alterations.

In the present investigation, ZnO nanoparticles were prepared by microwave-assisted synthesis method and stabilized with different capping agents such as sodium hexametaphosphate (SHMP), polyvinylpyrrolidone (PVP), and cetylpyridinium chloride (CPC). Furthermore, their photocatalytic degradation efficiency was examined by the degradation of methylene blue (MB) under visible light exposure.

Experimental section

Materials

Zinc sulphate, zinc acetate, zinc nitrate, NaOH, sodium hexametapolyphosphate (SHMP), polyvinylpyrrolidone (PVP), and cetylpyridinium chloride (CPC) material were sourced from Sigma-Aldrich. All these chemicals and reagents were utilized as received.

Synthesis of ZnO nanoparticles

ZnO nanoparticles were synthesized by using the microwave irradiation method. Herein, 0.5 mmol of zinc sulfate was taken in a beaker containing 100 mL of deionized (DI) water, to this mixture 0.5 N NaOH was added with constant stirring at room temperature and the mixture was subjected to microwave irradiation at 400w for 30 min (Mostafa et al. 2015). Finally, the obtained white precipitate (ZnO) was washed with water and ethanol several times followed at about 200 °C for 10–15 min. For the same product, a similar procedure was followed with different precursors such as zinc acetate and zinc nitrate with identical reaction conditions.

Synthesis of SHMP-, PVP-, and CPC-capped ZnO nanoparticles

For this, firstly 0.5 mmol of zinc sulphate was dissolved in 100 mL of distilled water followed by the addition of 1 wt% of SHMP capping agent, and to this mixture, 0.5 N of NaOH solution was introduced dropwise with constant stirring for 15 min. Finally, the solution mixture was irradiated in the microwave for 30 min. Then the formed precipitate was filtered, washed with water and ethanol, and dried at 200 °C for 10–15 min and is presented in Fig. 1. The above procedure is followed for the prepare PVP capped ZnO and CPC capped ZnO nanoparticles from the different precursors such as zinc acetate and zinc nitrate.

Material characterization

Samples of the present investigation were characterized with an XRD instrument manufactured by Bruker (Advance D8 X-ray diffractometer). The Cu Kα radiation ($\lambda = 1.5406$ Å) was used as the source of X-rays and the diffraction patterns

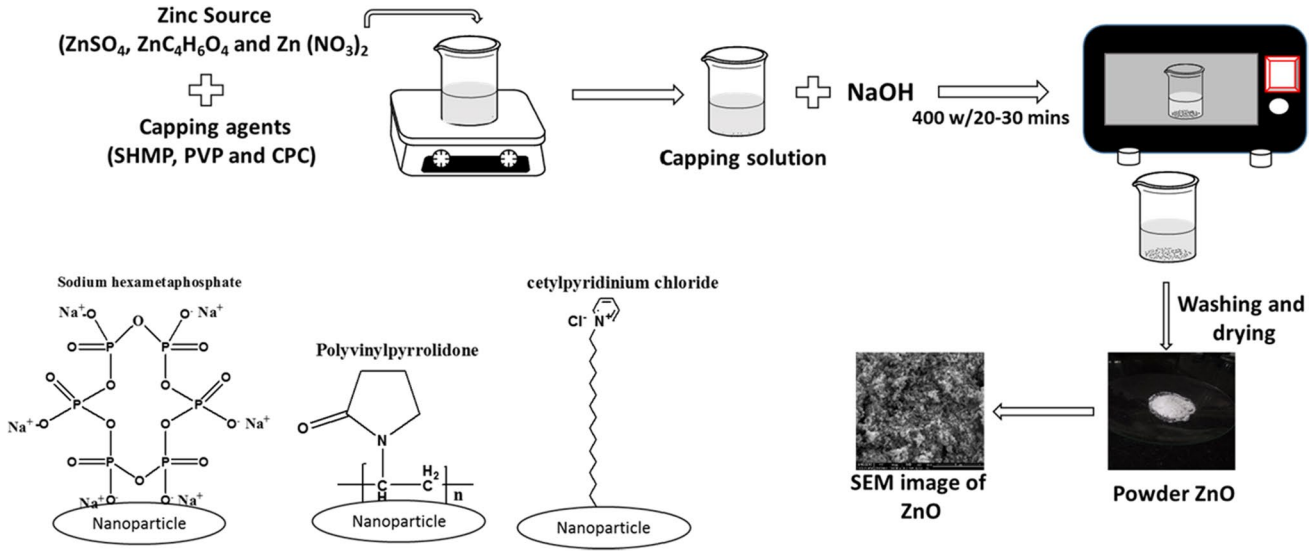

Fig. 1 Schematic illustration for the synthesis route of SHMP, PVP and CPC capped ZnO nanoparticles

were recorded in the 2θ range between 10 and 80° with a step size of 0.02°. The functional groups of synthesized ZnO nanomaterials were analyzed by the Fourier transformation spectrometer Spectrum 2000, Perkin Elmer. The UV–Vis diffuse reflectance spectrum was performed by JASCO V-630 UV/Vis spectrophotometer in the range 200–800 nm.

The surface morphology was acquired by SEM (JSM7600) and its corresponding elemental compositions were evaluated from EDS.

Photocatalytic degradation studies

The photocatalytic efficiency of the ZnO nanoparticles was assessed by the photo-degradation of MB under visible light irradiation. A 250 W tungsten halogen lamp was used as the irradiation source. In a typical photocatalytic degradation experiment, 75 mg of ZnO nanoparticles were added to 75 mL of the MB (2×10^{-4} M) and Tetracycline (TC) (3×10^{-5} M) in a cylindrical glass vessel. Prior to the light illumination, the suspension was placed at dark to attain adsorption equilibrium. At the time of light irradiation, 5 mL of the suspension was drawn and centrifuged to remove the catalyst after that the concentration of the solution was analysed at their absorption maximum (λ_{max}) at 664 and 353 nm for MB and TC respectively, using UV–Vis spectrophotometer (JASCOV-630).

Results and discussion

XRD analysis

Figure 2 shows the XRD patterns of the synthesized ZnO nanoparticles from (a) zinc sulphate, (b) zinc acetate, and (c) zinc nitrate precursors with different capping agents. As seen in Fig. 2 the XRD pattern of ZnO shows the diffraction peaks at 2θ = 31.9°, 34.7°, 36.5°, 47.7°, 56.8°, 63.0°, 66.3°, 67.9°, 69.1°, 73.1, and 77.0° and corresponds to (100), (002), (101), (102), (110), (103), (200), (112), (201), (004), and (202) diffraction planes (Katiyar et al. 2020). It is found to be well indexed with a hexagonal phase structure well with the standard JCPDS Card No. 00–005-0664.

From Fig. 2 (a–c), the peak intensity of the pure ZnO is majorly influenced by the addition of SHMP, PVP and CPC capping agents, the decrease in peak intensity was observed in the case of capping agents. Furthermore, Table 1 shows the crystalline sizes, microstrain, and FWHM values of the prepared ZnO with different capping agents.

This reveals that there is a decrease in the crystalline size while varying the capping agent with different zinc sources was noticed. TEM analysis showed that there was a strong link between these results as shown in Fig. 8.

FTIR studies

FTIR is one of the useful techniques to understand the nature of the functional groups present in the synthesized material. The unique vibrations of the bonds at different wavenumbers make this technique so powerful. The FTIR spectra of pure (ZnO) nanoparticles synthesized from different sources such as zinc nitrate with different capping agents are shown in Fig. 3. And FTIR spectra of zinc sulphate and zinc acetate are shown in Fig.S1 and S2, respectively. In Fig. S1 and S2, the FTIR spectra of pure (ZnO) show various peaks belonging to different functional groups such as Zn–O

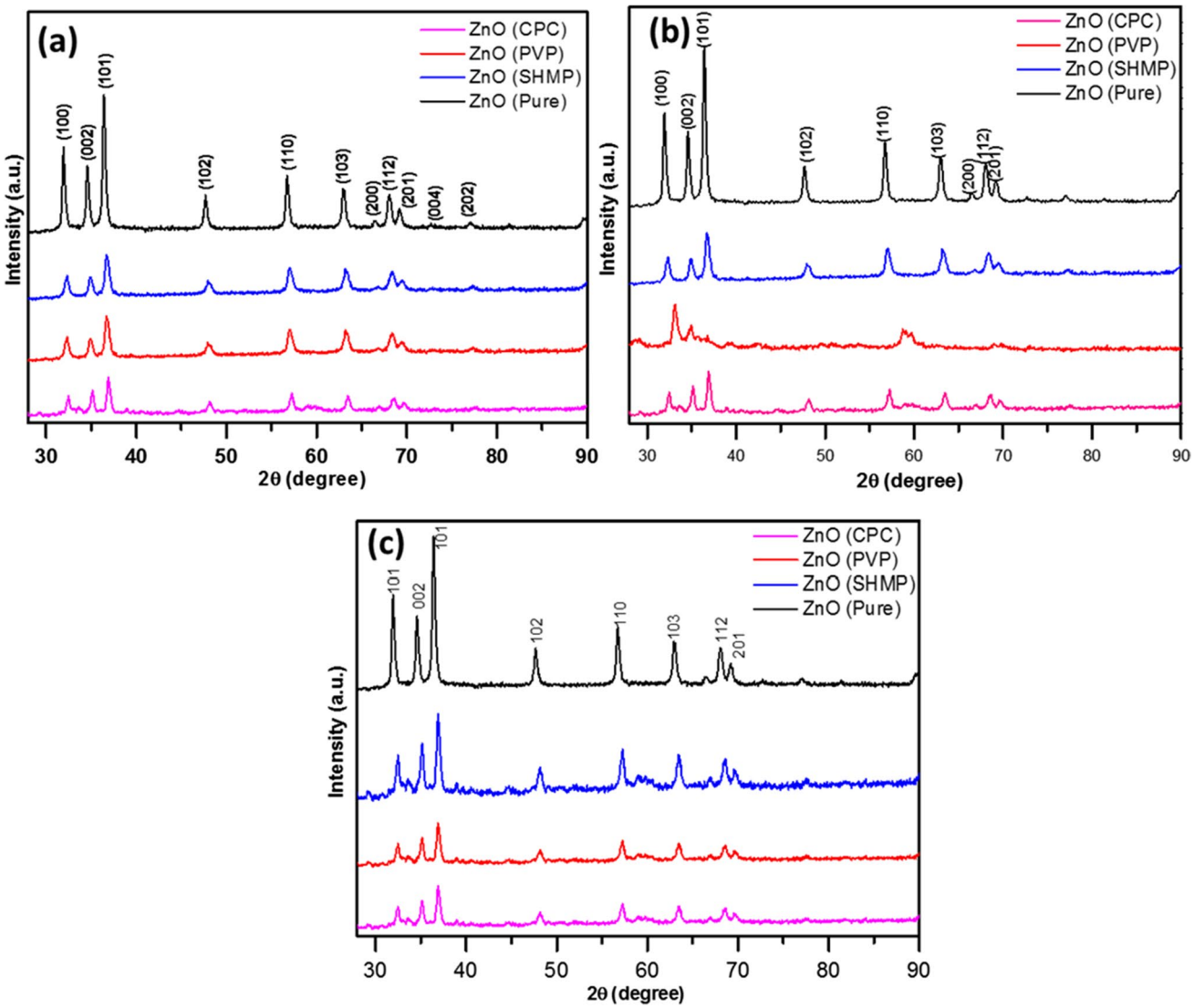

Fig. 2 XRD spectra of various capping agents (SHMP, PVP, and CPC) in the presence of **a** zinc sulphate, **b** zinc acetate, and **c** zinc nitrate

Table 1 The FWHM, interplanar spacing (d_{hkl}), crystallite size, microstrain and dislocation density of synthesized ZnO

Samples	FWHM of XRD peak (200)	d-spacing	Crystalline size (nm)	Micro-strain($\times 10^{-3}$)	Dislocation density ($\times 10^{14}$ lines/m^2)
Zinc sulphate (pure)	0.3653	2.47	48.042	7.2	4.3
SHMP	0.4173	2.42	35.469	9.7	7.9
PVP	0.0638	2.42	23.224	14.9	18.5
CPC	0.5438	2.42	27.245	12.7	13.4
Zinc acetate (pure)	0.6524	2.65	21.255	16.3	22.1
SHMP	0.1075	2.65	14.492	2.5	47.6
PVP	0.7986	2.62	18.164	1.9	30.3
CPC	0.6524	2.65	21.255	16.3	22.1
Zinc nitrate (pure)	0.4172	2.42	34.387	10.0	8.3
SHMP	0.3559	2.46	48.923	7.0	4.2
PVP	0.3619	2.46	48.125	7.2	4.3
CPC	0.5438	2.43	28.180	1.2	12.5

stretching observed between 560 and 450 cm^{-1}, symmetrical stretching and bending vibration of O–H appeared at 3600 and 1560 cm^{-1} respectively. The ZnO nanoparticles capped with different capping agents had different bands at different wavenumbers, and these bands represent the functional groups of the capping agents. Figure 3, S1 and S2 illustrate the reaction between different ZnO sources with SHMP, where the band for phosphate (–P = O) at 1110–150 cm^{-1} and phosphate oxygen group (P–O–P) appear at 800–900 cm^{-1}. For the PVP capping agent, the carbonyl group (C = O) peaks appeared at 1600–1700 cm^{-1}. Furthermore, absorption peaks appeared at 1200–1300 cm^{-1} confirming the presence of C–N linkage. The FTIR of CPC shows the appearance of a CH_2 peak at 2800–3000 cm^{-1} and appearance of C = C at 1600–1700 cm^{-1} and C–N linkage peak at 1300–1200 cm^{-1}. The coexistence of SHMP, PVP, and CPC in zinc source photocatalysts was found by FT-IR analyses.

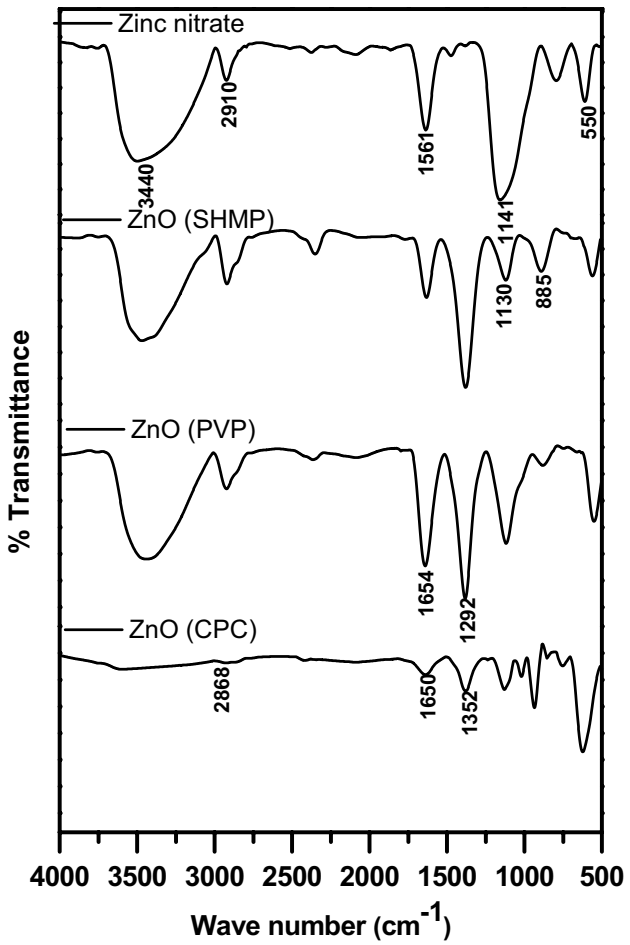

Fig. 3 FT-IR spectra of various capping agents (SHMP, PVP, and CPC) in the presence of Zinc nitrate

UV–visible studies

By using UV–vis DRS, the band gap energy value of ZnO nanoparticles from various sources and with various capping agents was examined the findings are displayed in Fig. 4. In Fig. 4, we assumed that the ZnO nanoparticles showed strong bands at 280 nm with sharp band edges (Prabukanthan and Harichandran 2013). Additionally, a slight hump is seen between 350 and 390 nm when various capping agents are combined with ZnO nanoparticles. This may be due to the bandgap increases (blue shift) with the addition of different capping agents. The increase in bandgap can be attributed to the slight difference in size and shape of ZnO nanoparticles from different sources with incorporation of different capping agents (Debanath and Karmakar 2013) respectively. This is because they absorb more of the visible light spectrum, which lets them work better as photocatalysts.

Photoluminescence spectrum and photoelectrochemical studies

Figure 5 depicts the photoluminescence (PL) spectra of ZnO nanoparticles synthesised from various sources and with various capping agents. It has two emission peaks in the UV region near band edge emission (NBE) and a defect-related green-orange band in the visible region. The NBE is primarily caused by the radiative recombination of excitons (an intrinsic property of wurtzite ZnO), whereas several types of defects, including zinc vacancies, oxygen vacancies, zinc interstitials, and adsorbed molecules, are responsible for the broad defect-related emission (Barick et al. 2015.). The resulting emissions of these defects are typically visible in the (610–750 nm) range (Pramanik et al. 2020.). This could be because the intensity of broad defect emission increases with the addition of different capping agents. Among various zinc sources, the PL intensity of ZnO/SHMP (Zinc nitrate) nanoparticles showed lower intensity than the pure ZnO and other zinc sources, which revealed that the recombination rate of photo-induced charge carriers is extremely reduced in ZnO/SHMP nanoparticles.

Photoelectrochemical experiments were carried out in order to determine the charge transfer (CT) capability of the photoinduced charge carriers in the prepared materials. The photocurrent response of pure ZnO and SHMP/ZnO nanoparticles with three on–off cycles are shown in Fig. 6a. The SHMP/ZnO nanoparticle demonstrated a superior photocurrent response than pure ZnO, which reveals the increase in the charge-separation efficiency of ZnO/SHMP nanoparticles.

The electrochemical impedance spectroscopy (EIS) measurements were carried out to govern the interfacial CT rate

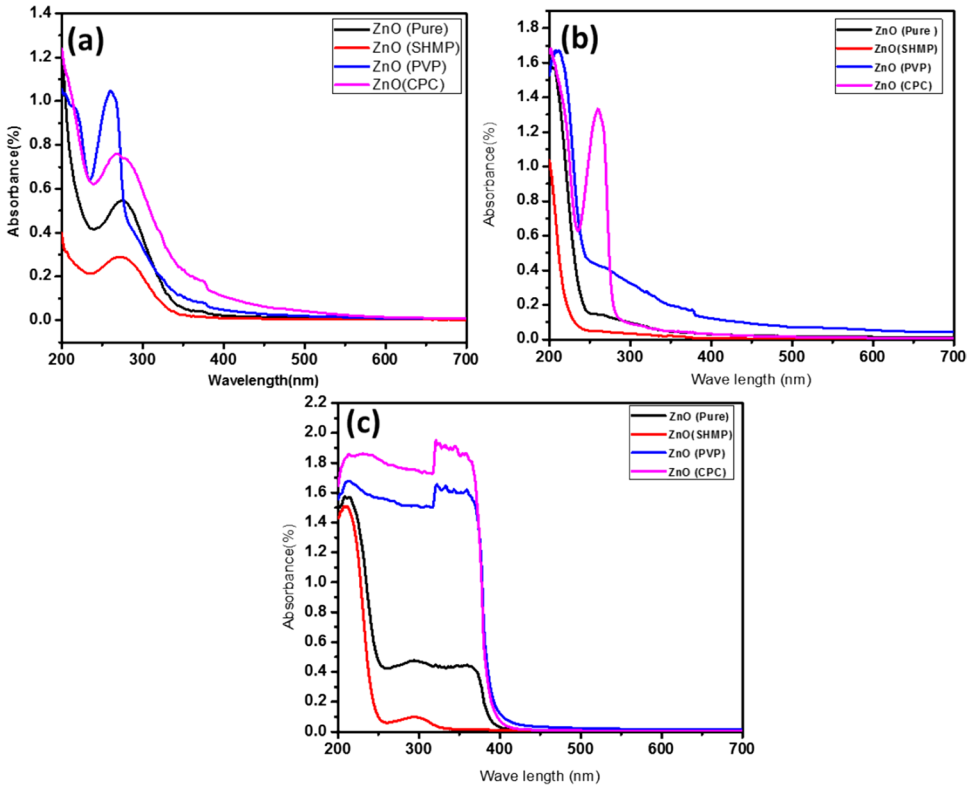

Fig. 4 UV spectra of various capping agents (SHMP, PVP, and CPC) in the presence of **a** zinc sulphate, **b** zinc acetate, and **c** zinc nitrate

of the pure ZnO and SHMP/ZnO nanoparticles, and the corresponding Nyquist plots are shown in Fig. 6b. The SHMP/ZnO has exhibited a smaller semicircular arc radius than that of the pure ZnO which exposes the good conductivity of SHMP/ZnO photocatalyst. As a result, the SHMP/ZnO exhibits greater charge separation efficiency, which is a vital quality for better photocatalytic activity.

Raman studies

Raman analysis was performed for all synthesized ZnO nanoparticles and the Raman spectra of ZnO nanoparticles with different capping agents synthesized from zinc sulfate, zinc acetate and zinc nitrate are shown in Fig. 7. The peak around 100 cm^{-1} is due to the E2 (low) of the ZnO nanoparticles. The pure ZnO nanoparticles exhibited a peak at 430 cm^{-1}, which corresponds to the E2 (high) mode of the wurtzite structure of the ZnO nanoparticles (Silambarasan et al. 2015.). The peak at 430 cm^{-1} was found in all other ZnO nanoparticles capped with different capping agents. The peak at 1000 cm^{-1} is due to the defects in the zone boundary phonons, which may be IR active and appear in the Raman (Sharma et al. 2012.). However, other peaks were found that could be associated with the capping agents. Similar observations were made in the Raman spectra of other ZnO nanoparticles synthesized from zinc acetate and zinc nitrate sources.

This implies that the SHMP, PVP, and CPC are linked through various zinc sources. This coupling could be important because it prevents charge carriers from recombining and has a synergistic impact on boosting photocatalytic activity.

Morphological analysis

The morphology of all the samples was examined with SEM and TEM are shown in Fig. 8 and Fig. S3. From Fig. 8 and Fig. S3, we can see the surface morphology of the synthesized pure ZnO has an agglomerated spherical structure. Similar observations were found in SEM studies for ZnO nanoparticles synthesized from zinc acetate and zinc nitrate (Ahammed et al. 2020) (see Fig. 8 (i) and Fig. S3a (i)-b(i)). The morphology with the presence of different capping agents for all samples, namely zinc sulfate, zinc acetate, and zinc nitrate, is shown in Fig. 8 (ii-iv) and Figure S3a(ii-iv)-b(ii-iv). It can be seen that the ZnO/SHMP (zinc sulphate, zinc acetate, and zinc nitrate) has well-dispersed nanocrystals whose spherical morphology (Fakhari et al. 2019.) can be seen in Fig. 8a (ii) and S3a(ii)-b(ii). PVP/ZnO (zinc sulphate, zinc acetate, and zinc nitrate) shows the formation of rice grain-like structures (Shaba et al. 2021), shown in Fig. 8(iii) and S3a(iii)-b(iii). In the case of CPC/ZnO (zinc sulphate, zinc acetate, and zinc nitrate), the structures of the microspheres are uniformly and homogeneously distributed

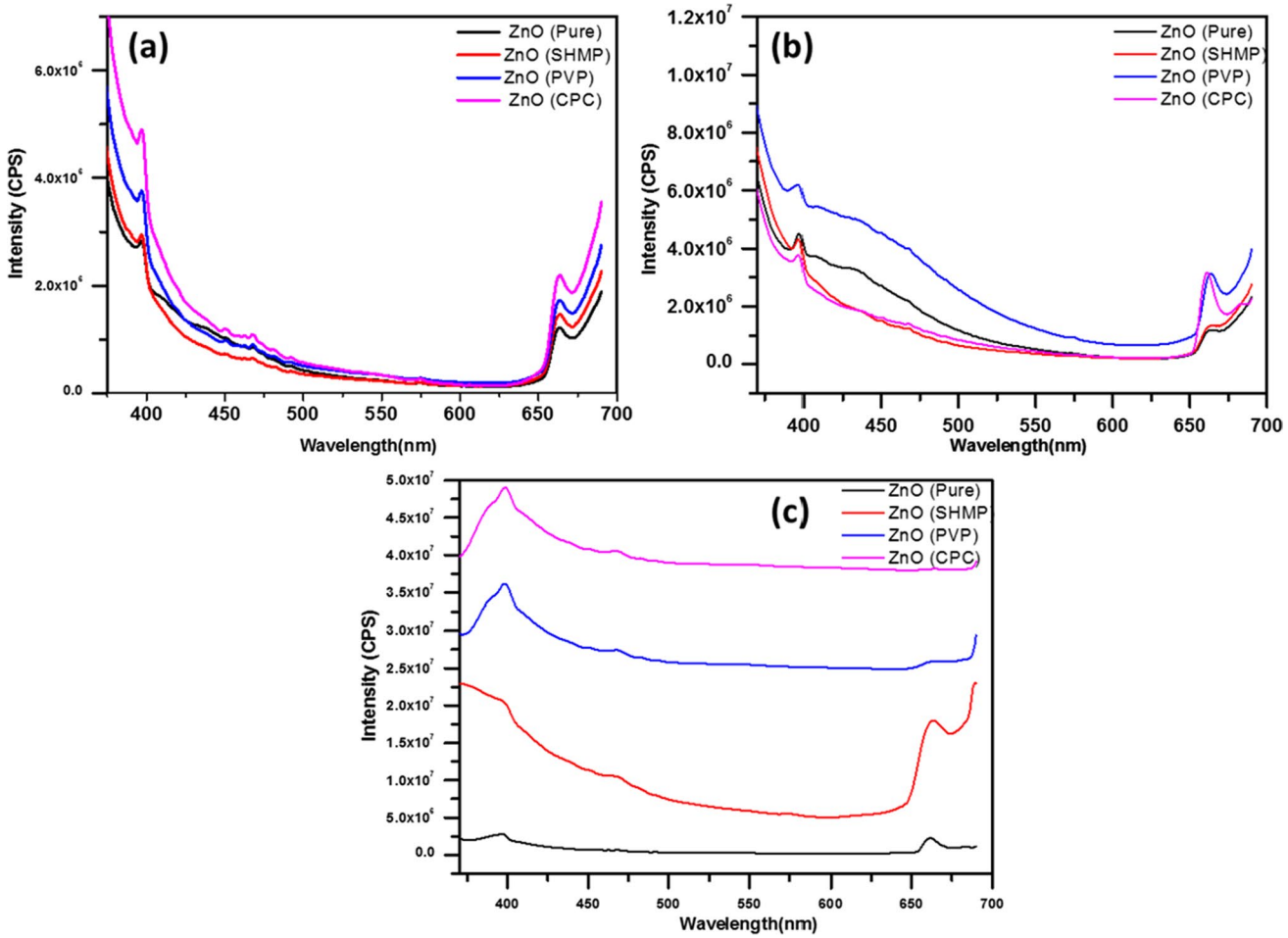

Fig. 5 Photoluminescence spectra of various capping agents (SHMP, PVP, and CPC) in the presence of **a** zinc sulphate, **b** zinc acetate, and **c** zinc nitrate

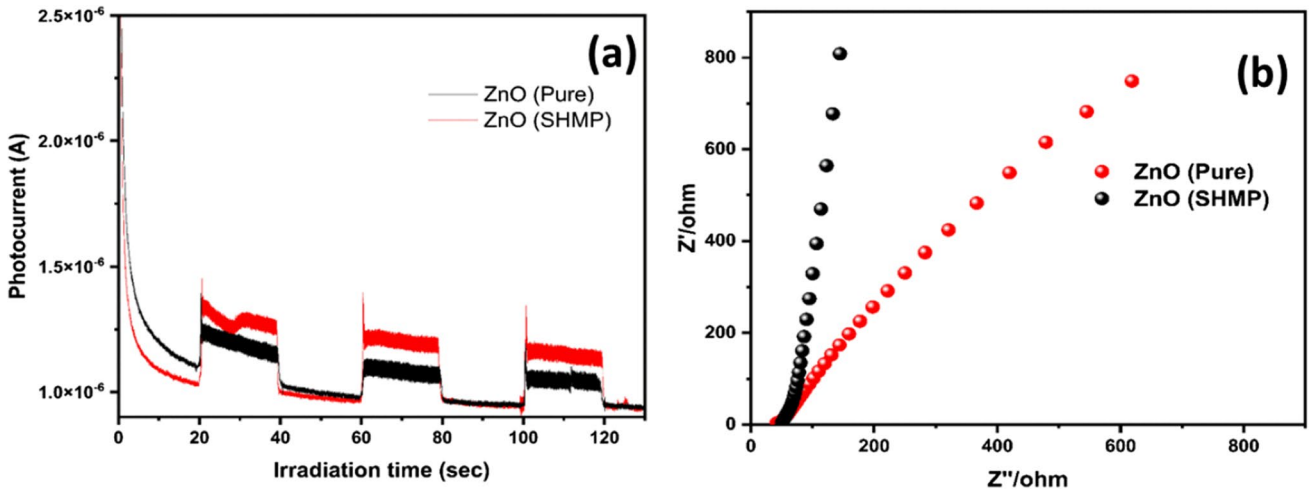

Fig. 6 **a** Transient-photocurrent curves for the pure ZnO and ZnO/SHMP nanoparticle photocatalysts with different on–off cycles of visible light irradiation. **b** Nyquist plots of the pure ZnO and ZnO/SHMP nanoparticle photocatalysts

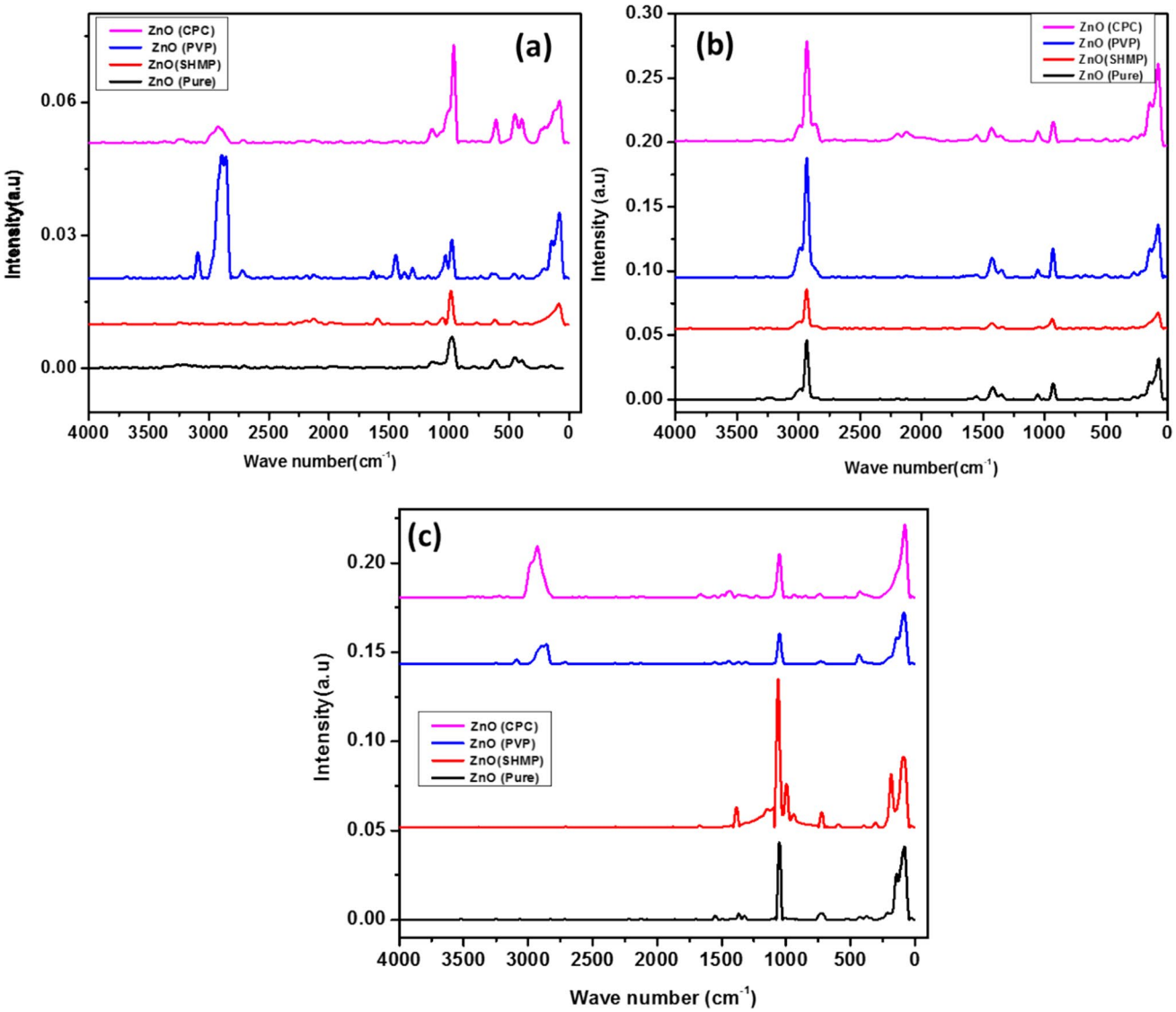

Fig. 7 Raman spectra of various capping agents (SHMP, PVP, and CPC) in the presence of **a** zinc sulphate, **b** zinc acetate, and **c** zinc nitrate

(Kaenphakdee et al. 2022) (Fig. 8(iv) and Figure S3a(iv iv)). Furthermore, HR-TEM analysis is used to determine the distribution and presence of SHMP on the surface of ZnO nanoparticles, and the findings are shown in Fig. 8b, c, and d. The HRTEM image clearly showed that the SHMP spheres were evenly distributed on the surface of the ZnO nanoplates. When ZnO/SHMP nanoparticles are present, it is likely that there will be more reactive sites that can trap charge carriers and attract different dye species to their surfaces shown in Fig. 8d. Furthermore, HR-TEM of optimized ZnO/SHMP reveals the SHMP on the surface of ZnO nanoparticles, and the findings are shown in Fig. 8. It can be evidenced that the Zn, P, and O element mapping images were detected for optimised ZnO/SHMP nanoparticle (Fig. 8e) respectively.

The results also indicate that the degree of agglomeration becomes weaker with increasing concentration of the capping agent (Stevanović et al. 2011). The ZnO nanoparticles with SHMP, PVP and CPC capping agents exhibited smaller particle sizes and uniform shapes compared to ZnO (Javed et al. 2016). This may be due to the high surface energy leading to their enlargement and instability. A mechanism involves the formation of a strong covalent bond between the surfaces of the nanoparticles and the polymer chains (Nguyen et al. 2014). In other words, the different sizes and shapes of the ZnO nanoparticles caused by the capping agents are due to the structural variation and surface coordination of the molecules of the capping agent with ZnO (Baig et al. 2021). This evidence is well supported by TEM results shown in Fig. 8.

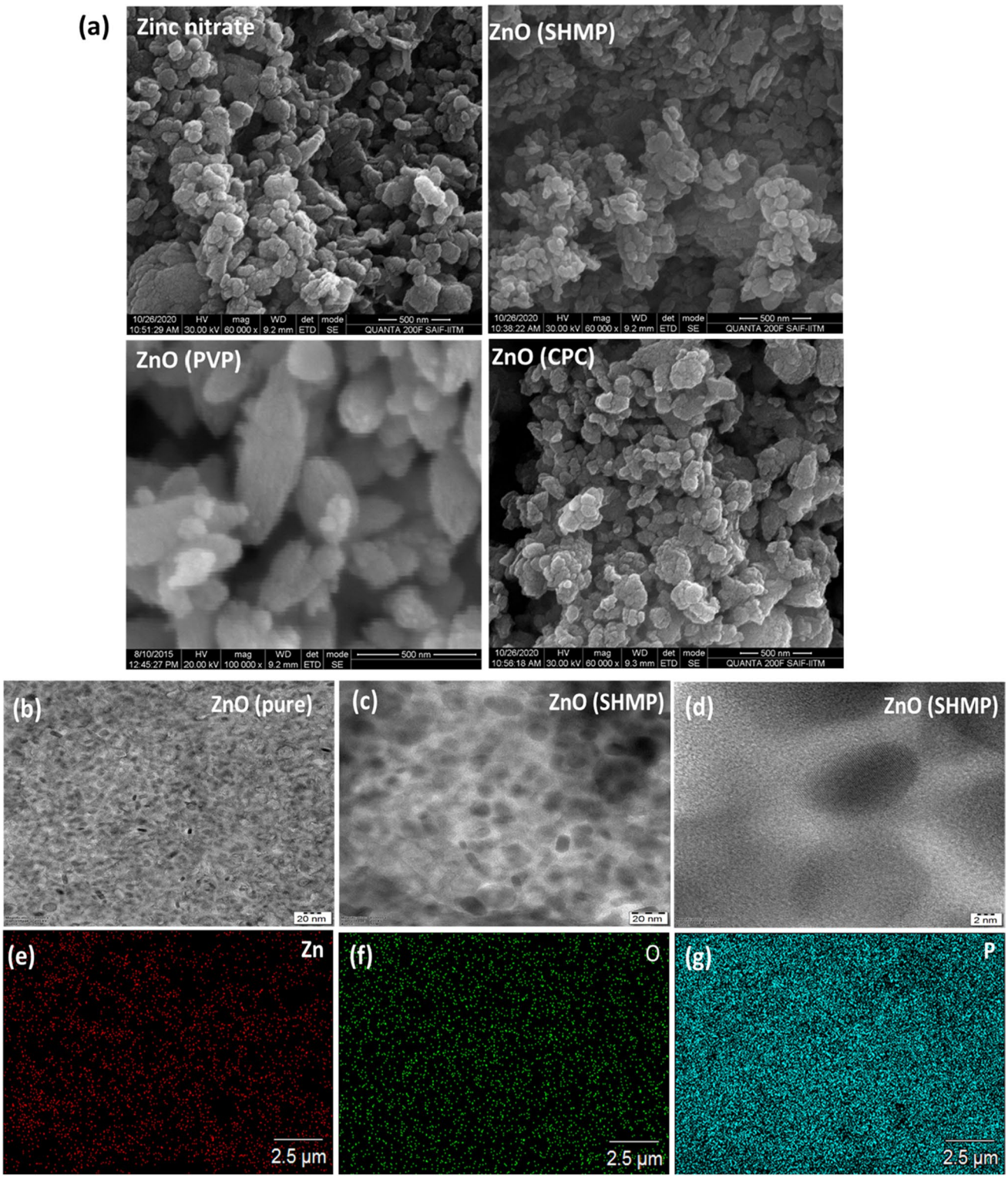

Fig. 8 **a** SEM images of various capping agents (SHMP, PVP, and CPC) in the presence of zinc nitrate source, TEM images of pure ZnO (**b**), ZnO/SHMP nanoparticle (**c**-**d**). HRTEM image of ZnO/SHMP nanoparticle with Elemental mapping (**e**-**g**)

Photocatalytic degradation studies

The photocatalytic degradation ability of synthesized ZnO nanoparticles from different sources with three capping agents has been investigated by the degradation of MB under visible light irradiation. The respective degradation plots are shown in Fig. 9. It is observed that the photo-degradation efficiency of ZnO nanoparticles synthesized

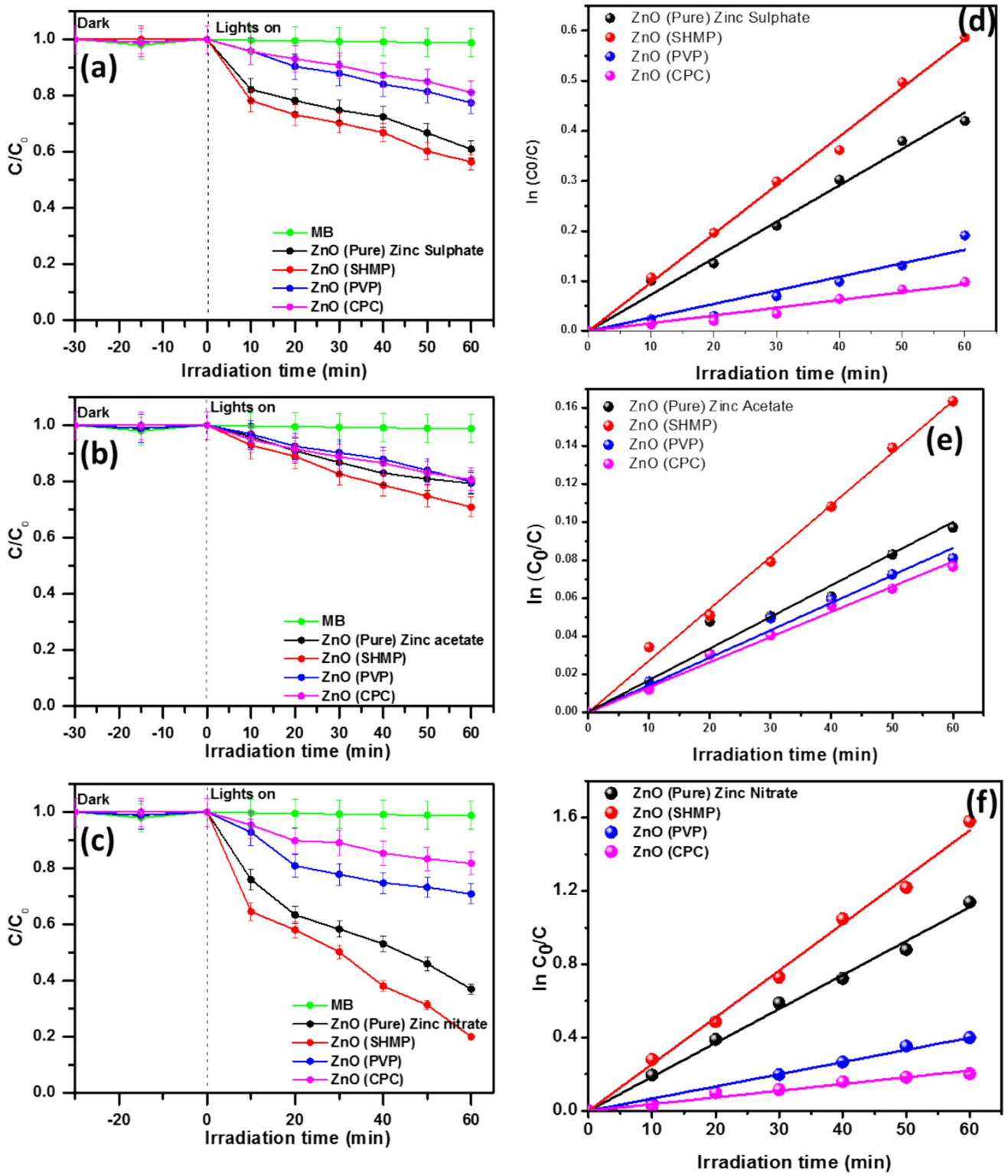

Fig. 9 Photocatalytic activity of ZnO prepared from precursors **a** zinc sulphate, **b** zinc acetate, and **c** zinc nitrate and various capping agents (SHMP, PVP, and CPC). **d**–**f** Their respective kinetic plots of photocatalytic degradation. (All experiments are carried out thrice and their average values are plotted)

Table 2 Comparison of photocatalytic performance of the various ZnO catalyst

Photocatalyst	Pollutant	Photocatalytic efficiency (%)	Irradiation time (min)	References
Cd:Ag:ZnO: PVP	MB	99	120	Vignesh et al.2019
Dalbergia parviflora capped ZnO	RR	95	120	Tammanoon et.al. 2022
Gly@ ZnO NPs (GZ2)	RhB	99	60	Basnet, P, et al.2020
ZnO NPs using C edulis	CR	97	130	J. Fowsiya, et.al.2017
PVP capped ZnO	CR	99	120	Chankhanittha,et al. 2019
ZnO-Bi_2WO_6	CIP	85	120	Chankhanittha et al. 2021
ZnO/CdS	RR	73	240	Senasu, et al. 2020
Pithecellobium dulce/ZnO	MB	63	120	Madhumitha et al. 2019
ZnO/ SHMP	MB	80	60	Present work

MB, methylene blue; *CIP*, ciprofloxacin; *RR*, Reactive red 141; *CR*, Congo red; *RhB*, Rhodamine B

from zinc nitrate has a higher degradation efficiency compared to the other two zinc sources selected in this study. The degradation efficiency of ZnO nanoparticles from zinc sulphate and zinc acetate was less than 50%. The pure (ZnO) and capped ZnO nanoparticles from zinc sulphate and zinc acetate sources had not shown the expected photodegradation efficiency, which could be due to the size of the ZnO nanoparticles (Basnet et al. 2019; Sharma

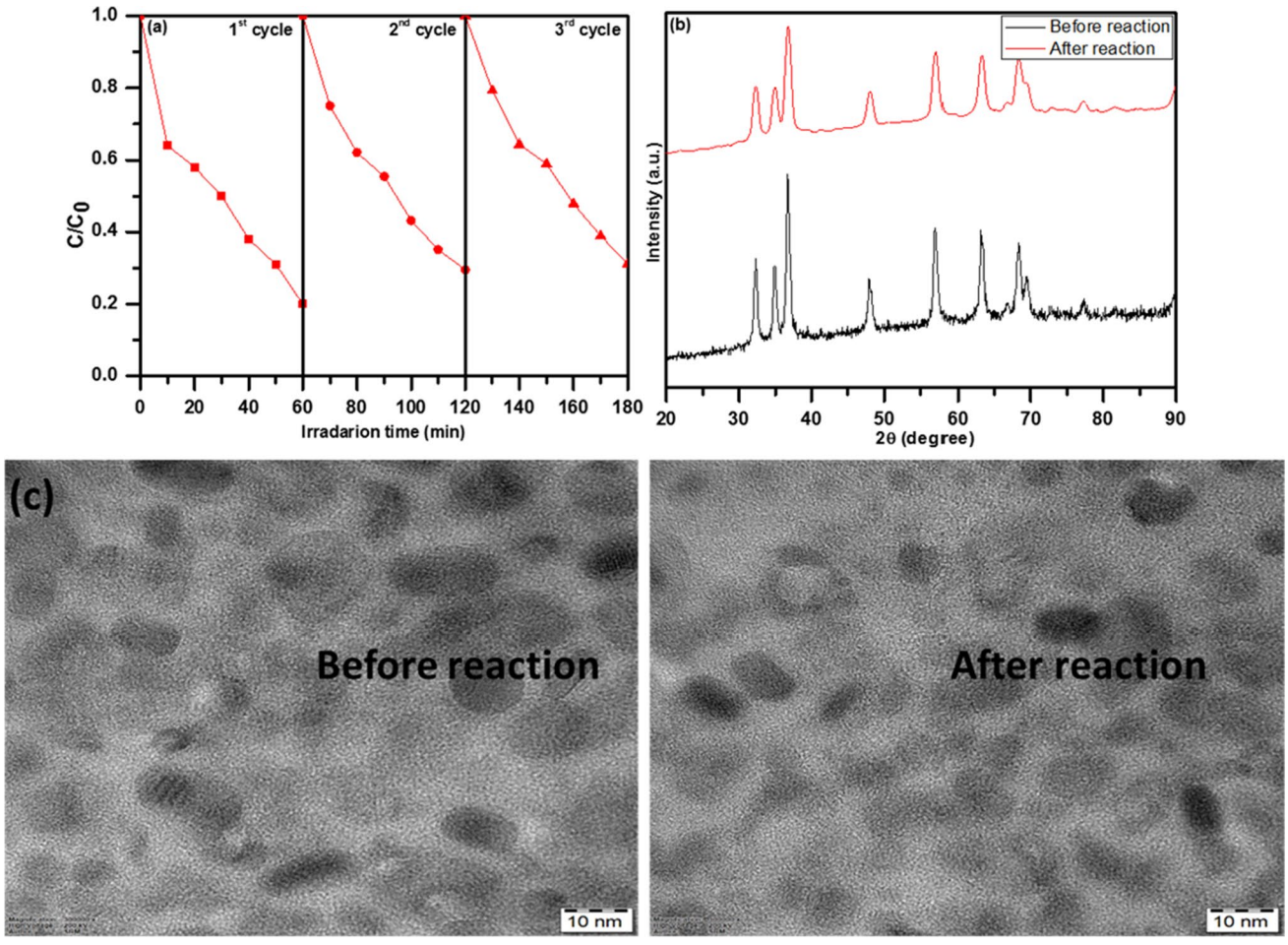

Fig. 10 **a** Recycling test results for the photocatalytic degradation of MB in VLI over the optimized ZnO/SHMP nanoparticle. **b** XRD patterns and **c** TEM image of before and after recycling test of the ZnO/SHMP nanoparticles

et al. 2020). The superiority of ZnO nanoparticles from zinc nitrate is due to the smaller particle size compared to the other two sources. The smaller the particles, the larger their surface area, and the more MB are adsorbed on the surface and degraded by light. Interestingly, not all ZnO nanoparticles from the nitrate source showed maximum efficiency. The degradation efficiency of ZnO capped with PVP and CPC is found very low. The ZnO nanoparticles capped with SHMP were superior to the degradation of MB with an efficiency of 80%, while the uncapped ZnO had an efficiency of 60%. The difference in efficiency between the capping agents could be due to the activation of surface sites for the adsorption of MB for photodegradation (Mohamed et al. 2022). PVP and CPC might have blocked and inactivated the surface-active sites of ZnO for the adsorption of MB, resulting in lower degradation efficiency compared to uncapped and SHMP-capped ZnO (Singh et al. 2015). This demonstrates that the interfacial charge-transfer and separation efficiency of photoexcited charge carriers is greater for ZnO/SHMP nanoparticles, which are highly desirable due to their superior photocatalytic properties (Fig. 11). These results highlight the potential of SHMP-ZnO nanoparticles to efficiently degrade MB under visible light irradiation. As well the photocatalytic activity of the optimized catalyst was evaluated for the photocatalytic degradation of tetracycline (TC) under VLI is depicted in Fig. S4. In Fig. S4, we can infer the stable nature of TC in visible light from the blank experimental result in the absence of a photocatalyst.

It can further be observed that there was no significant tetracycline photolysis until 60 min of illumination, which revealed that the TC is relatively stable under light irradiation. Figure S4 presents the photodegradation of tetracycline over pure ZnO and ZnO/SHMP nanoparticles which degrade ~ 49 and 33% of the TC after 60 min of VLI. Furthermore, it can be seen that the SHMP/ZnO nanoparticle revealed superior photocatalytic activity than that of the pure photocatalyst prepared without any capping agent. Table 2 compares the photocatalytic performance of the various ZnO catalyst.

Photostability and reusability studies

To investigate the photostability and reusability of the ZnO/SHMP nanoparticle, three cycling experiments of MB photodegradation under visible-light illumination (VLI) have been performed. At the end of each cycle, the catalyst has been collected by centrifugation and dried at 80 °C for 6 h. Then it was reintroduced into the next cycle. Figure 10a presents the three recycling runs of ZnO/SHMP nanoparticles over the degradation of MB under VLI. From Fig. 10a, it can be seen that the photocatalytic activity of the ZnO/SHMP nanoparticle is stable even after three cycling runs, revealing the strong photostability and reusability capabilities of the as-synthesized ZnO/SHMP nanoparticle. Furthermore, the ZnO/SHMP nanoparticle employed in the cycling tests is characterized using XRD before and after the experiments. The XRD patterns in Fig. 10b reveal no considerable changes were observed before and after recycling experiments of the ZnO/SHMP nanoparticle. This evidence is well supported by TEM results (Fig. 10c). These findings demonstrated that ZnO/SHMP nanoparticles have strong photostability and reusability capabilities, which are critical for their practical applicability in pollutant degradation research.

Photocatalytic degradation mechanism

Figure 11 depicts the photocatalytic degradation mechanism of MB using pure zinc sources and various capping agents. When exposed to ultraviolet light, electrons in the valence band (VB) become excited and migrate to the conduction band (CB), leaving behind holes (h^+) in the VB. Electrons can activate molecular oxygen to make superoxide radicals and anion $O_2^{\cdot -}$, whereas photogenerated holes (h^+) can either combine with water (H_2O) or $OH^{\cdot -}$ produce $OH^{\cdot}$. Both $OH^{\cdot}$ and $O_2^{\cdot -}$ are strong radicals.

This promotes the suppression of charge carrier recombination, resulting in the ZnO/SHMP nanoparticles having a more efficient photocatalytic property than other photocatalytic materials (Tayyab et al. 2022a; Bavani et al. 2022). The entire photocatalytic reactions under VLI are depicted in Fig. 11.

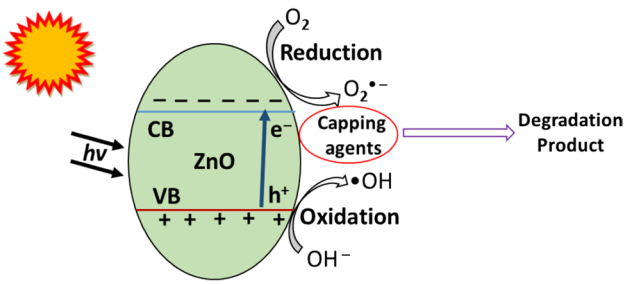

Fig. 11 Pictorial representation of mechanism for the degradation of MB over ZnO nanoparticle under VLI

Conclusion

In the present study, the ZnO nanoparticles have been successfully synthesized from different zinc sources by microwave irradiation method. Moreover, the ZnO nanoparticles were capped with three different capping agents such as SHMP, PVP, and CPC. The synthesized ZnO nanoparticles were well characterized by means of XRD, UV-DRS, PL, FTIR, and Raman analysis and their results are discussed well.

The photodegradation studies confirmed the superiority of ZnO nanoparticles prepared from zinc nitrate over other precursors, with the highest photocatalytic efficiency achieved (80% degradation in 60 min) when stabilized with SHMP than other capping agents and zinc sources. These results suggest that zinc nitrate is a suitable source for the synthesis of ZnO nanoparticles. Based on the results of the photocatalytic activity, stability, and reusability tests, the ZnO/SHMP nanoparticle is recommended as a promising material for pollutant degradation and other environmental remediation applications.

Supplementary Information The online version contains supplementary material available at https://doi.org/10.1007/s11356-022-25097-9.

Author contribution Kumar Mageswari: funding acquisition, investigation, methodology, writing—original draft, visualization, data curation. Peethambaram Prabukanthan: supervision, funding acquisition, investigation, methodology, project administration, writing—original draft, review and editing, visualization, data curation. Jagannathan Madhavan: validation, writing—review and editing.

Data availability Data are not available.

Declarations

Ethical approval The study did not include human or animal subjects; therefore, ethical approval is not required.

Consent to participate This manuscript has no human experiments (not applicable).

Consent to publish This manuscript has no human experiments (not applicable).

Competing interestss1 The authors declare no competing interests.

References

Ahammed KR, Ashaduzzaman Md, Shujit Paul C, Nath MR, Snahasish Bhowmik S, Saha O, Mizanur Rahaman Md, Bhowmik S, Aka TD (2020) Microwave assisted synthesis of zinc oxide (ZnO) nanoparticles in a noble approach: utilization for antibacterial and photocatalytic activity. SN Appl Sci 2:955. https://doi.org/10.1007/s42452-020-2762-8

Ameen F, Dawoud T, AlNadhari S (2021) Ecofriendly and low-cost synthesis of ZnO nanoparticles from Acremonium potronii for the photocatalytic degradation of azo dyes. Environ Res 202:111700. https://doi.org/10.1016/j.envres.2021.111700

Arumugam S, Bavani T, Preeyanghaa M, Alaswad SO, Neppolian B, Madhavan J, Murugesan S (2022) A facile synthesis of visible light driven Ni3V2O8 nano-cube/BiVO4 nanorod composite photocatalyst with enhanced photocatalytic activity towards degradation of acid orange 7. Chemosphere 308:136100. https://doi.org/10.1016/j.chemosphere.2022.136100

Baig N, Kammakakam I, Falathabe W (2021) Nanomaterials: a review of synthesis methods, properties, recent progress, and challenges. Mater Adv 2:1821–1871. https://doi.org/10.1039/D0MA00807A

Barick KC, Sharma P, Mukhija A, Sainis JK, Gupta A, Hassan PA (2015) Effect of cetylpyridinium chloride on surface passivation and photocatalytic activity of ZnO nanostructures. J Environ Chem Eng 3:1346–1355. https://doi.org/10.1016/j.jece.2014.12.007

Basnet P, Dhrubajyoti Samanta T, Chanu I, Mukherjee J, Chatterjee S (2019) Assessment of synthesis approaches for tuning the photocatalytic property of ZnO nanoparticles. SN Appl Sci 1:633. https://doi.org/10.1007/s42452-019-0642-x

Basnet P, Samanta D, Chanu TI, Jha S, Chatterjee S (2020) Glycine-A bio-capping agent for the bioinspired synthesis of nano-zinc oxide photocatalyst. J Mater Sci: Mater Electron 31:2949–2966. https://doi.org/10.1007/s10854-019-02839-z

Bavani T, Madhavan J, Preeyanghaa M, Neppolian B, Murugesan S (2022) Construction of direct Z-scheme g-C_3N_4/$BiYWO_6$ heterojunction photocatalyst with enhanced visible light activity towards the degradation of methylene blue. Environ Sci Pollut Res. https://doi.org/10.1007/s11356-022-22756-9

Bhuvaneswari K, Palanisamy G, Sivashanmugan K, Pazhanivel T, Maiyalagan T (2021) ZnO nanoparticles decorated multiwall carbon nanotube assisted ZnMgAl layered triple hydroxide hybrid photocatalyst for visible light-driven organic pollutants removal. J Environ Chem Eng 9:104909. https://doi.org/10.1016/j.jece.2020.104909

Chandrappa KG, Venkatesha TV (2012) Electrochemical synthesis and photocatalytic property of zinc oxide nanoparticles. Nano-Micro Lett 4(1):14–24. https://doi.org/10.1007/BF03353686

Chankhanittha T, Watcharakitti J, Nanan S (2019) PVP-assisted synthesis of rod-like ZnO photocatalyst for photodegradation of reactive red (RR141) and Congo red (CR) azo dyes. J Mater Sci: Mater Electron 30:17804–17819. https://doi.org/10.1007/s10854-019-02132-z

Chankhanittha T, Somaudon V, Photiwat T, Youngme S, Hemavibool K, Nanan S (2021) Enhanced photocatalytic performance of ZnO/Bi2WO6 heterojunctions toward photodegradation of fluoroquinolone-based antibiotics in wastewater. J Phys Chem Solids 153:109995. https://doi.org/10.1016/j.jpcs.2021.109995

Chankhanittha T, Yenjai C, Nanan S (2022) Utilization of formononetin and pinocembrin from stem extract of Dalbergia parviflora as capping agents for preparation of ZnO photocatalysts for degradation of RR141 azo dye and ofloxacin antibiotic. Catal Today 384–386:279–293. https://doi.org/10.1016/j.cattod.2021.03.002

Chauhan PS, Kant R, Rai A, Gupta A, Bhattacharya S (2019) Facile synthesis of ZnO/GO nanoflowers over Si substrate for improved photocatalytic decolorization of MB dye and industrial wastewater under solar irradiation Mater. Sci Semicond Process 89:6–17. https://doi.org/10.1016/j.mssp.2018.08.022

Debanath MK, Karmakar S (2013) Study of blueshift of optical band gap in zinc oxide (ZnO) nanoparticles prepared by low-temperature wet chemical method. Mater Lett 111:116–119. https://doi.org/10.1016/j.matlet.2013.08.069

Fakhari S, Jamzad M, Fard KH (2019) Green synthesis of zinc oxide nanoparticles: a comparison. Green Chem Lett Rev 12:19–24. https://doi.org/10.1080/17518253.2018.1547925

Flores NM, Pal U, Galeazzia R, Sandoval A (2014) Effects of morphology, surface area, anddefect content on the photocatalytic dye degradation performance of ZnO nanostructures. RSC Adv 4:41099–41110. https://doi.org/10.1039/C4RA04522J

Fowsiya J, Madhumitha G, Al-Dhabi NA, ValanArasu M (2016) Photocatalytic degradation of Congo red using Carissa edulis extract capped zinc oxide nanoparticles. J Photochem Photobiol, B 162:395–401. https://doi.org/10.1016/j.jphotobiol.2016.07.011

Hsu CL, Chen KC, Tsai TY, Hsueh TJ (2013) Fabrication of gas sensor based on p-type ZnO nanoparticles and n-type ZnO nanowires. Sens Actuators B 182:190–196. https://doi.org/10.1016/j.snb.2013.03.002

Huang R, Wu J, Zhang M, Liu B, Zheng Z, Luo D (2021) Strategies to enhance photocatalytic activity of graphite carbon nitride-based photocatalysts. Mater Des 210:110040. https://doi.org/10.1016/j.matdes.2021.110040

Javed R, Usman M, Tabassum S, Zia M (2016) Effect of capping agents: Structural, optical and biological properties of ZnO nanoparticles. Appl Surf Sci 386:19–326. https://doi.org/10.1016/j.apsusc.2016.06.042

Kaenphakdee S, Putthithanas P, Yodyingyong S, Leelawattanachai J, Triampo W, Sanpo N, Jitputti J, Triampo D (2022) Zinc oxide synthesis from extreme ratios of zinc acetate and zinc nitrate: synergistic morphology. Materials (basel) 13:570. https://doi.org/10.3390/ma15020570

Katiyar A, Kumar N, Shukla RK, Srivastava A (2020) Influence of alkali hydroxides on synthesis, physico-chemical and photoluminescence properties of zinc oxide nanoparticles. Materials Today: Proceedings 29:885–889. https://doi.org/10.1016/j.matpr.2020.05.112

Lv Y, Guo L, Xu H, Chu X (2007) Gas-sensing properties of well-crystalline ZnO nanorods grown by a simple route. Physica E 36:102–105. https://doi.org/10.1016/j.physe.2006.09.014

Madhumitha G, Fowsiya J, Gupta N, Kumar A, Singh M (2018) Green synthesis, characterization and antifungal and photocatalytic activity of Pithecellobium dulce peel–mediated ZnO nanoparticles. J Phys Chem Solids 127:43–51. https://doi.org/10.1016/j.jpcs.2018.12.005

Mohamed NBH, Ouni S, Bouzid M, Bouzidi M, Petricioletd AB, Haouari M (2022) Adsorption and photocatalytic degradation of an industrial azo dye using colloidal semiconductor nanocrystals. https://doi.org/10.21203/rs.3.rs-1057236/v2.

Mostafa NY, Heiba ZK, Ibrahim MM (2015) Structure and optical properties of ZnO produced from microwave hydrothermal hydrolysis of tris(ethylenediamine)zinc nitrate complex. J Mol Struct 1079:480–485. https://doi.org/10.1016/j.molstruc.2014.09.059

Murali A, Sarswat PK, Sohn HY (2019) Enhanced photocatalytic activity and photocurrent properties of plasma-synthesized indium-doped zinc oxide nanopowder. Mater Today Chem 11:60–68. https://doi.org/10.1016/j.mtchem.2018.10.007

Nguyen TK, Thanh MN, Mahiddine S (2014) Mechanisms of nucleation and growth of nanoparticles in solution. Chem Rev 114:7610–7630. https://doi.org/10.1021/cr400544s

Pascariu P, Tudose IV, Suchea M, Koudoumas E, Fifere N, Airinei A (2018) Preparation and characterization of Ni, Co doped ZnO nanoparticles for photocatalytic applications. Appl Surf Sci 448:481–488. https://doi.org/10.1016/j.apsusc.2018.04.124

Prabukanthan P, Harichandran G (2013) Effect of 100 MeV O^{7+} ion beam irradiation on radio frequency reactive magnetron sputtered ZnO thin films. Mater Sci Semicond Process 16:193–199. https://doi.org/10.1016/j.mssp.2012.04.016

Pramanik S, Mondal S, Mandal AC, Mukherjee S, Das S, Ghosh T, Nath R, Manoranjan G, Kuiri PK (2020) Role of oxygen vacancies on the green photoluminescence of microwave-assisted grown ZnO nanorods. J Alloy Compd 849:156684. https://doi.org/10.1016/j.jallcom.2020.156684

Rout L, Aniket Kumar L, Achary SK, Barik B, Dash P (2019) Ionic liquid assisted combustion synthesis of ZnO and its modification by AuSn bimetallic nanoparticles: an efficient photocatalyst for degradation of organic contaminants. Mater Chem Phys 232:339–353. https://doi.org/10.1016/j.matchemphys.2019.04.063

Samadi M, Zirak M, Naseri A, Khorashadizade E, Moshfegh AZ (2016) Recent progress on doped ZnO nanostructures for visible-light photocatalysis. Thin Solid Films 605:2–19. https://doi.org/10.1016/j.tsf.2015.12.064

Senasu T, Chankhanittha T, Hemavibool K (2021) Nanan S (2021) Visible-light-responsive photocatalyst based on ZnO/CdS nanocomposite for photodegradation of reactive red azo dye and ofloxacin antibiotic. Mater Sci Semicond Process 123:105558. https://doi.org/10.1016/j.mssp.2020.105558

Senasu T, Chankhanittha T, Hemavibool K, Nanan S (2020) Visible-light-responsive photocatalyst based on ZnO/CdS nanocomposite for photodegradation of reactive red azo dye and ofloxacin antibiotic. Mater Sci Semicond Process 105558.https://doi.org/10.1016/j.mssp.2020.105558

Shaba EY, Jacob JO, Tijani JO, Suleiman MAT (2021) A critical review of synthesis parameters affecting the properties of zinc oxide nanoparticle and its application in wastewater treatment. Appl Water Sci 11:48. https://doi.org/10.1007/s13201-021-01370-z

Sharma A, Singh BP, Dhar S, Gondorf A, Spasova M (2012) Effect of surface groups on the luminescence property of ZnO nanoparticles synthesized by sol–gel route. Surf Sci 606(3–4):L13–L17. https://doi.org/10.1016/j.susc.2011.09.006

Sharma R, Garg R, Kumari A (2020) A review on biogenic synthesis, applications and toxicity aspects of zinc oxide nanoparticles. Excli J 19:1325–1340. https://doi.org/10.17179/excli2020-2842

Silambarasan M, Saravanan S, Soga T (2015) Raman and photoluminescence studies of Ag and Fe-doped ZnO nanoparticles. Int J ChemTech Res 73:1644–1650

Singh NK, Saha S, Pal A (2015) Solar light-induced photocatalytic degradation of methyl red in an aqueous suspension of commercial ZnO: a green approach. Desalination Water Treatment 53(2):501–514. https://doi.org/10.1080/19443994.2013.838520

Stevanović M, Kovačević B, Petković J, Filipič M, Uskoković D (2011) Effect of poly-α, γ, L-glutamic acid as a capping agent on morphology and oxidative stress-dependent toxicity of silver nanoparticles. Int J Nanomedicine 6:2837–2847. https://doi.org/10.2147/IJN.S24889

Tayyab M, Liu Y, Liu Z, Pan L, Xu Z, Yue W, Zhou L, Lei J, Zhang J (2022) One-pot in-situ hydrothermal synthesis of ternary In2S3/Nb2O5/Nb2C Schottky/S-scheme integrated heterojunction for efficient photocatalytic hydrogen production. J Colloid Interface Sci 628:500–512. https://doi.org/10.1016/j.jcis.2022.08.071

Tayyab M, Liu Y, Min S, Irfan RM, Zhu Q, Zhou L, Lei J, Zhang J (2022) Simultaneous hydrogen production with the selective oxidation of benzyl alcohol to benzaldehyde by a noble-metal-free photocatalyst VC/CdS nanowires. Chinese J Catal 43(4):1165–1175. https://doi.org/10.1016/S1872-2067(21)63997-9

Tiwari A, Khan SA, Kher RS (2012) Study of size dependent photoluminescence properties of copper doped sodium hexametaphosphate capped ZnS nanoparticles. J Lumin 132:1564–1567. https://doi.org/10.1016/j.jlumin.2012.01.036

Vignesh S, Suganthi S, Sundar JK, Raj V, Devi PI (2019) Highly efficient visible light photocatalytic and antibacterial performance of PVP capped Cd:Ag: ZnO photocatalyst nanocomposites. Appl Surf Sci 479:914–929. https://doi.org/10.1016/j.apsusc.2019.02.064

Zamirin R, Kaushal A, Rebelo A, Ferreira JMF (2014) Er doped ZnO nanoplates: Synthesis, optical and dielectric properties. Ceram Int 40:1635–1639. https://doi.org/10.1016/j.ceramint.2013.07.054

Zhu D, Zhou Q (2019) Action and mechanism of semiconductor photocatalysis on degradation of organic pollutants in water treatment: a review. Environ Nanotechnol Monit Manag 12:100255. https://doi.org/10.1016/j.enmm.2019.100255